2

RADC-TR-90-389
Final Technical Report
December 1990

AD-A232 552

PULSE COMPRESSION OF 100 PICOSECOND PULSES AT 1.319 MICRONS

University of Arizona

Jason P. Sokoloff, Steven T. Johns, Mark F. Krol, John L. Stacy

APPROVED FOR PUBLIC RELEASE; DISTRIBUTION UNLIMITED.

Rome Air Development Center
Air Force Systems Command
Griffiss Air Force Base, NY 13441-5700

This report has been reviewed by the RADC Public Affairs Division (PA) and is releasable to the National Technical Information Service (NTIS). At NTIS it will be releasable to the general public, including foreign nations.

RADC-TR-90-389 has been reviewed and is approved for publication.

APPROVED:

ANDREW R. PIRICH, Chief
Analog Optical & Lightwave
Signal Processing Division
Photonics Laboratory

APPROVED:

DONALD W. HANSON
Director of Surveillance & Photonics

FOR THE COMMANDER:

BILLY G. OAKS
Directorate of Plans & Programs

REPORT DOCUMENTATION PAGE

Form Approved
OMB No. 0704-0188

1. AGENCY USE ONLY (Leave Blank)	2. REPORT DATE	3. REPORT TYPE AND DATES COVERED
	December 1990	Final May 89 to May 90

4. TITLE AND SUBTITLE
PULSE COMPRESSION OF 100 PICOSECOND PULSES AT 1.319 MICRONS

5. FUNDING NUMBERS
C - F30602-88-D-0026
PE - 62702F
PR - 4600
TA - P2
WU - P4

6. AUTHOR(S)
Jason P. Sokoloff, Steven T. Johns, Mark F. Krol, John L. Stacy

7. PERFORMING ORGANIZATION NAME(S) AND ADDRESS(ES)
University of Arizona
Optical Sciences Center
Tucson AZ 85721

8. PERFORMING ORGANIZATION REPORT NUMBER
D. O. No. 0013

9. SPONSORING/MONITORING AGENCY NAME(S) AND ADDRESS(ES)
Rome Air Development Center (OPA)
Griffiss AFB NY 13441-5700

10. SPONSORING/MONITORING AGENCY REPORT NUMBER
RADC-TR-90-389

11. SUPPLEMENTARY NOTES
RADC Project Engineer: John L. Stacy/OPA/(315) 330-2937. The prime contractor for this effort is Calspan-UB Research Center, P.O. Box 400, Buffalo NY 14225.

12a. DISTRIBUTION/AVAILABILITY STATEMENT
Approved for public release; distribution unlimited.

12b. DISTRIBUTION CODE

13. ABSTRACT (Maximum 200 words)

This report describes the fiber-grating pair optical pulse compression set-up at the Photonics Laboratory, Griffiss AFB NY, which compresses 110-120 picosecond (ps) pulses, with 1.319 micron (um) wavelength, down to 1-2 ps.

14. SUBJECT TERMS
Pulse Compression, Group Velocity Dispersion (GVD)

15. NUMBER OF PAGES
24

16. PRICE CODE

17. SECURITY CLASSIFICATION OF REPORT	18. SECURITY CLASSIFICATION OF THIS PAGE	19. SECURITY CLASSIFICATION OF ABSTRACT	20. LIMITATION OF ABSTRACT
UNCLASSIFIED	UNCLASSIFIED	UNCLASSIFIED	UL

I. Introduction

A facility providing temporally short pulses is extremely useful for investigating the limitations of optical detectors, or signal processing networks. For instance, two picosecond (ps) pulses have a 500 GHz bandwidth and can therefore be used in experimental systems designed for operation one to two orders of magnitude faster than those presently in use. This report describes the fiber-grating pair optical pulse compression set-up at the Photonics Center in Rome, NY which compresses 110-120 picosecond pulses, with a 1.319 micron (μm) wavelength, down to 1-2 ps. The exact temporal width of these pulses is measured by an autocorrelator.

It is easy to compress pulses with a wavelength < 1.32 (μm) if they have the following qualities a) their spectral bandwidth is larger than the inverse of their temporal pulse width and b) the instantaneous frequency varies linearly across the pulse (i.e. it has a linear chirp). In a fiber-grating pair compression stage the light pulse is first coupled into a fiber. Two processes, which will be explained briefly, transform the pulse so that it has the above two qualities. Self-phase-modulation (SPM) broadens the pulse spectrally satisfying (a), and group-velocity dispersion (GVD) broadens the pulse temporally. When the optimum fiber length for the given input pulse is chosen, the output pulse has a linear chirp. At this point the pulse is sent through a dispersive delay line with anomalous GVD, which exactly compensates for the fiber imposed linear chirp. When the pulse emerges from the delay line, which in our case is a grating pair, the "red" wavelengths at the leading edge of the pulse are delayed just enough to let the "blue" wavelengths at the trailing edge of the pulse catch up. The net result is a large temporal compression of the pulse.

The report begins with a very brief theoretical background on pulse compression and then gives the step-by-step procedure for setting such a system up. Following the pulse compression segment is a short description of the autocorrelator which was built to measure the temporal width of these pulses.

II. Theoretical Background

The next several sections follow closely the presentation in parts of Chapters 1, 2, 3, 4, and 6 of *Nonlinear Fiber Optics* by G. P. Agrawal (Academic Press, 1989). First the basic propagation equation of a pulse in a fiber is set forth. This equation contains terms responsible for both temporal pulse broadening (GVD), and spectral broadening (SPM). Additionally, using this equation it is easy to see why a linear chirp becomes imposed on the pulse.

A. The Propagation Equation

The electric field of a pulse propagating down a fiber can be written

$$\underline{E}\,(\underline{r},t) = \frac{1}{2}\{F(x,y)\;A(z,t)\;\exp[i(\beta_0 z - \omega_0 t)] + c.c.\} \tag{1}$$

Here F(x,y) is the transverse mode, A(z,t) is the slowly varying amplitude of the pulse envelope which enters the fiber at z=0, ω_0 and β_0 are the pulse envelope carrier frequency and carrier wavenumber, respectively, and c.c. stands for complex conjugate. By including nonlinear polarization source terms in the wave equation, it can be shown that the slowly varying amplitude of the pulse envelope A(z,t) satisfies

$$\frac{\partial A}{\partial z} + \beta_1 \frac{\partial A}{\partial t} + \frac{i}{2}\beta_2 \frac{\partial^2 A}{\partial t^2} + \frac{\alpha}{2}A = i\gamma|A|^2 A \;. \tag{2}$$

The coefficients β_1 and β_2 take into account the dispersion of the wavenumber $\beta(\omega)$ as a function of frequency, that is

$$\beta(\omega) = \beta_0 + (\omega - \omega_0)\beta_1 + \frac{1}{2}(\omega - \omega_0)^2\beta_2 + \ldots$$

Physically β_1 is related to the pulse group velocity v_g, $\beta_1 = \frac{1}{v_g}$, and β_2 is related to the GVD, $\beta_2 = \left(\frac{\partial\beta_1}{\partial\omega}\right) = \frac{1}{v_g^2}\frac{dv_g}{d\omega}$. α and γ in the above equation take into account absorption losses in the fiber, and nonlinearities respectively ($\alpha = n_2\omega_0/cA_{eff}$) where c is the speed of light, n_2 is the intensity dependent part of the refractive index, and A_{eff} is the effective core area).

Equation (2) can be rewritten in normalized units. First define a time scale in the reference frame of the moving pulse which is normalized to the initial pulse width T_0,

$$\tau = \frac{t - z/v_g}{T_0} = \frac{T}{T_0}$$

Also, normalize the pulse amplitude to the incident peak power P_0

$$A(z,\tau) = \sqrt{P_0}\,\exp(-\alpha z/2)\; u(z,\tau)$$

The propagation equation (Eq. (2)) becomes

$$i\frac{\partial u}{\partial z} = \frac{\mathrm{sgn}(\beta_2)}{2L_D}\,\frac{\partial^2 u}{\partial \tau^2} - \frac{\exp(-\alpha z)}{L_{NL}}\,|u|^2 u \tag{4}$$

where $\mathrm{sgn}(\beta_2) = \pm 1$, depending on the sign of β_2, $L_D = \frac{T_0^2}{|\beta_2|}$, and $L_{NL} = \frac{1}{\alpha P_0}$. L_D and L_{NL} are length scales over which dispersive or nonlinear effects become important in the pulse evolution. In what follows each term in the RHS of Eq. (4) will be considered separately also, since we are interested in the "normal" dispersion regime of optical fibers we use $\mathrm{sgn}(\beta_2) = +1$.

B. Group Velocity Dispersion (GVD)

The fiber can be considered as a linear dispersive medium by setting $\gamma = 0$ in Eq. (4). Then Eq. (4) becomes

$$i\frac{u}{\partial z} = \frac{1}{2}\beta_2\,\frac{\partial^2 u}{\partial T^2} \tag{5}$$

The Fourier Transform of Eq. (5) is

$$i\frac{\partial \tilde{u}}{\partial z} = -\frac{1}{2}\beta_2 \omega_2\,\tilde{u}$$

which has the solution

$$\tilde{u}(z,\omega) = \tilde{u}(0,\omega)\,\exp\left(\frac{i}{2}\beta_2\omega^2 z\right) . \tag{6}$$

So at a point z in the fiber

$$u(z,T) = \frac{1}{2\pi}\int_{-\infty}^{\infty} d\omega\; \tilde{u}(0,\omega)\,\exp i(\beta_2\omega^2 z - \omega T)$$

where

$$\tilde{u}(0,\omega) = \int_{-\infty}^{\infty} u(0,T)\, e^{+i\omega T}\, dT$$

Equation (6) shows that at a point z each *spectral* component is the same as at z=0, *except* for a phase factor $e^{i\phi}$ where $\phi = \beta_2\omega^2 z/2$. This phase factor not only changes the input temporal pulse shape, but gives it a frequency chirp also.

Gaussian Pulse Example

Consider a Gaussian input pulse (z=0) which has the form

$$u(0,T) = \exp\left(-\frac{T^2}{2T_0^2}\right)$$

Using Eq. (6) we see that the linear dispersive fiber changes its shape to

$$u(z,T) = \frac{T_0^2}{T_0^2 - i\beta_2 z} \exp\left[\frac{T^2}{2(T_0^2 - i\beta_2 z)}\right].$$

Notice that $T_0^2 \rightarrow T_1^2 = T_0^2 \left(1 + \frac{z}{L_D}\right)^2$ (recall $z/L_D = |\beta_2| z/T_0^2$). Since $T_1^2 > T_0^2$ then the pulse height is reduced and the pulse becomes *temporally* broader. Also, by writing u(z,T) as an imaginary number

$$u(z,T) = u_r(z,T) + u_{im}(z,T)$$

$$= |u(z,T)|\, e^{i\phi(z,T)}$$

we find that the instantaneous frequency across the pulse varies *linearly* with T

$$\Delta\omega = -\frac{\partial\phi}{\partial T} = \frac{2(z/z_0)}{T_0^2(1 + (z/L_D)^2)}\, T \ .$$

The pulse now has a linear chirp as a result of the GVD. At the temporal center of the pulse (T=0) the instantaneous frequency is ω_0, but at a leading or trailing portion of the pulse (T≠0) the instantaneous frequency varies from ω_0 by $\delta\omega$ as given in the above equation.

C. Self Phase Modulation

Equation (4) shows that the propagation equation also has a term proportional to the normalized intensity, $|u|^2$. To see the effects of this term, we momentarily "turn off" the GVD effect by setting β_2=0. The propagation equation becomes

$$\frac{\partial u}{\partial z} = \frac{i}{L_{NL}} \exp(-\alpha z) \, |u|^2 \, u \tag{7}$$

which has the solution

$$u(z,T) = u(0,T) \exp(i\phi_{NL}(z,T)) \tag{8}$$

where

$$\phi_{NL}(z,T) = |u(0,T)|^2 \, \frac{z_{eff}}{L_{NL}} \tag{9}$$

Here z_{eff} is an effective fiber length that takes into account absorption loss, that is $z_{eff} = \frac{1}{\alpha}(1 - \exp(-\alpha z))$, and $\lim\limits_{\alpha \to 0} z_{eff} = z$.

From Eq. (9) we see that the instantaneous optical frequency varies across the temporal profile of the pulse from its central value ω_0. The amount it varies by, at T≠0 is

$$\Delta\omega(T) = \omega(T) - \omega(T = 0)$$

$$= -\frac{\partial \phi_{NL}}{\partial T} = -\frac{\partial}{\partial T} |u(0,T)|^2 \, \frac{z_{eff}}{L_{NL}} \tag{10}$$

On the other hand Eq. (8) shows that as the pulse propagates, its magnitude does not change; i.e. there is no temporal shape change. However, the phase of the pulse does vary with propagation distance z and intensity $|u|^2$, as is shown explicitly in Eq. (9). The consequence of this self phase modulation is that as the pulse propagates the spectral component at each point in the pulse varies by an increasingly larger amount from the component ω_0 at the center of the pulse.

Therefore, under the right conditions an incident pulse will undergo significant spectral broadening within a fiber.

In the above presentation, either GVD or SPM was considered separately, however both effects are always present and there is an interplay between them. For instance, because SPM generates a broader spectrum, GVD causes the pulse to spread out temporally more than if there were no SPM. This can result, in a pulse with a rectangular temporal profile, and linear chirp. Figure 3 shows an example of this.

The relative importance of GVD versus SPM can be determined by rewriting the propagation equation one more time as

$$i \frac{2}{\pi} \frac{\partial u}{\partial(z/z_0)} = \frac{1}{2} \frac{\partial^2 u}{\partial \tau^2} - N^2 e^{-\alpha z} |u|^2 u$$

where

$$z_0 = \frac{\pi}{2} L_D, \; \tau = \frac{T}{T_0} \text{ and}$$

$$N^2 = \frac{L_D}{L_{NL}} = \frac{\gamma P_0 T_0^2}{|\beta_2|} .$$

GVD dominates for $N^2 << 1$ and SPM for $N^2 >> 1$. At 1.319 μm typical values of γ and β_2 are $\gamma = \frac{20}{W{\cdot}km}$, $|\beta_2| = \frac{20\ ps^2}{km}$. For a 100 MHz modelocked YAG laser typical values of P_0 and T_0 are $P_0 = 100$ w, $T_0 = 100$ ps. So $N^2 = 10^6$ and SPM dominates as would be expected since 1.319 is so close to the zero dispersion wavelength γ_δ.

D. Grating Pairs

A grating pair with the proper configuration can act as a delay line with anomalous dispersion. The effective GVD parameter is

$$\beta_2^{eff} = -\frac{2a_c}{b_0}$$

where

$$a_c = \frac{4\pi c\ b_0}{\omega_0^3 \Lambda^2 \cos^2 \theta_{or}}$$

Here b_0 is the center to center spacing of the grating pair, Λ is the grating period, and all other quantities are either as defined earlier, or defined in figure 1. When the proper slant length b_0 is used, the grating pair compensates for the fiber induced linear chirp and the pulse emerging from the fiber-grating pair is compressed.

III. Fiber-Grating Pair Compressor Design

A. Useful Formulas

For a pulse with a given temporal width T_0, peak power P_0 and wavelength λ, it is useful to have formulas which guide in the fiber compression design. The needed quantities are a) optimum fiber length and b) grating pair separation. It is also useful to know c) the expected compression factor T_0/T_c.

a) Optimum fiber length z_{opt}

$$z_{opt} \simeq 1.6/N\ z_0$$

b) Slant length b_0 is derived from

$$\frac{a_c}{T_0^2} \simeq \frac{1.6}{N}$$

so

$$b_0 = \left[\frac{\omega_0^3\ d^2 \cos^2 \theta_{or}}{4\pi c}\right] \frac{1.6}{N} T_0^2$$

c) Compression factor $\frac{T_0}{T_c}$

$$\frac{T_0}{T_c} = \left[\frac{1.6}{N}\right]^{-1}$$

or

$$T_c = \frac{1.6}{N} T_0$$

If fiber lengths z are used which are much shorter than z_{opt}, the following formulas are used

$$b_0 = \frac{13}{84} \cdot \left\{ \frac{\omega_0^3 \, d^2 \cos^2 \gamma}{4\pi c} \right\} \frac{1.6}{N^2} \frac{z_0}{z} T_0^2$$

$$T_c \simeq \frac{T_0}{1 + 0.9N^2 \, (z/z_0)}$$

For example, typical cw-modelocked parameters for a pulse at 1.319 μm are T_0 = 110 ps, P_0 = 100 W. Typical parameters for a dispersion shifted fiber are $|\beta_2|$ = 20 ps²/km γ = 20/W·km. So z_0 = 950 km, N = 1.1 × 10^{+3} and using the above equations for $z \simeq z_{opt}$, we get z_{opt} = 1.4 km. For a grating with 1800 lines/mm and using γ_0 = 45° b_0 = 3 m.

B. Alignment Procedure

There are only two steps to aligning a fiber-grating pair pulse compressor. Step 1 is to select the fiber length, and step 2 is to set the slant length b_0. From the preceding example $z_{opt} \simeq$ 1.4 km and $b_0 \simeq$ 3 m. These are approximate values.

Choosing the right fiber length amounts to choosing a fiber length that results in an output pulse with a rectangular spectral and temporal shape. Therefore, a spectrum analyzer and sampling scope are helpful, but not absolutely necessary. As an alternative to adjusting the fiber length from its approximate value to optimum length for a given P_0, the fiber length can be kept constant and the input power P_0 can be varied either by using a $\lambda/2$ plate and polarizer, or a circular neutral density filter.

Here is the alignment procedure.

1. Couple into and out of the fiber with a 20X and 10X microscope objective, respectively. Use a power meter at the output; a ≥ 50% throughput is adequate.

2. Optimize the power through the fiber. This is done by noting at what power stimulated Raman scattering (SRS) just begins to appear, and can be observed in 3 ways:

   a) Bounce the output pulse off a grating and look at its first order spectrum using an IR viewer. The Raman line, which is due to a 330 cm^{-1} phonon mode of silica, will appear separate from the band centered around 1.319 μm.

b) Look at the output spectrum using a spectrum analyzer. The Raman line is at $\simeq$ 1.405 μm.

c) Look at the output pulse using a sampling oscilloscope. The Raman pulse will lead the main pulse.

A rule of thumb is that $\simeq$ 5% of the total intensity should be in the Raman line. Keeping this in mind, P_0 can be increased if the fiber is shortened.

3. Set the grating spacing; use a double pass configuration so that b_0 can be charged without transversely translating the grating pair output path. Adjust b_0 for the minimum pulse width by monitoring the temporal width using an autocorrelator. It may be necessary to coarsely adjust the grating spacing using a sampling scope and fast detector for the initial adjustment, and then use the autocorrelator for the final optimization.

IV. Autocorrelator

The *autocorrelator* is a modified Michaelson interferometer. A time variable delay is introduced by sending both beams through a rotating glass block $\simeq$ 7 mm thick. One beam is displaced vertically by a right angle prism before the two beams are recombined in the second harmonic doubling crystal. The flat retroreflecting mirror is mounted on a one-dimensional translation stage that is useful for calibrating the measurement screen of the oscilloscope displaying the autocorrelator trace.

V. Experimental Results

Figures 2 and 3 show actual experimental traces of the temporal and spectral profile of a 1.319 μm wavelength at different stages of a pulse compression setup. Figure 2 shows the initial pulse, which has a temporal width of 101 ps and a <1nm bandwidth. At the output of the fiber (figure 3) it has broadened both spectrally and temporally due to the nonlinear effects discussed earlier. The spectral content of the pulse has broadened to 3.5 nm and its intensity, as a function of wavelength, has the is fairly even distribution desired. The factor of two temporal broadening is comparable, but not equal to the broadening factor predicted by the above equations.

This is not surprising, since the above equations are actually intended as design guides rather than stringent design rules. More careful comparisons of theory and experiment must be done using beam propagation techniques (see Agrawal's book for an overveiw of such techniques). Presumably in figure 3b the long wavelength spectral spectral components of the pulse are at the front end of the pulse, the short wavelength components are at the back, and there is a linear variation in between. This could be checked by an elaborate setup such as a streak camera measurement where first the sampled pulse is sent through a dispersive (nonchirping) mechanism, such as a spectrometer. It could also be checked by taking a cross correlation measurement of the fiber output pulse with an already characterised compressed pulse. In this second method a diode array at the output of a spectrometer would detect the different (upconverted) components. The second method is doesn't require a streak camera so is much easier, but it is also of course redundant; if you have a well characterised compressed pulse why characterise for the sake of compression a second pulse of the same wavelength. For these reasons it is preferred, and more importantly, adequate to rely on the empirical techniques mentioned in the III B, to determine if the fiber output pulse has the proper spectral preparation.

In the setup which produced the traces of figures 2 and 3 it was sufficient to have an initial grating spacing which was within a factor of 3 of the final optimum spacing. This resulted in about a 20 ps pulse which was then gradually optimized to about 3 ps by adjusting slant length. Final adjustment to the observed 2 ps autocorrelation pulse was obtained by <2 changes in the pulse launch intensity. This measured pulse corresponds to an actual pulse width of about 1.3 ps once the 1.5 deconvolution factor (for gaussian pulses) is included.

It is worth mentioning that when the glass block is symmetrically situated to generate time delays in both beams, as in this case (see figure 4), the generated time delay versus angle change is linear over a surprisingly large range. This is confirmed by a simple ray diagram calculation. The useful range of the autocorrelator of course depends on the thickness of the glass block used as a delay line. Increasing the autocorrelator range of course means that the block will have to spin faster for live monitoring purposes. This puts higher demands on the mechanical components the autocorrelator, and increases the need for proper dynamic balancing. A smaller range (thinner block) is useful only once the system is near optimization. For a system producing 1-2 ps pulses a useful (i.e. linear) range of 20 ps seems to be adequate once the above tradeoffs are considered.

Appendix A: Useful Formulas

1. Factorized form of electric field in a fiber

$$E\left(\underset{-}{r}, t\right) = \frac{1}{2}\{F(x,y)\ A(z,t)\ \exp[i(\beta_0 z - \omega_0 t)] + c.c.\}$$

2. Propagation Eq. for slowly varying part of E(r,t)

$$\frac{\partial A}{\partial z} + \beta_1 \frac{\partial A}{\partial t} + i\beta_2 \frac{\partial^2 A}{\partial t^2} + \frac{\alpha}{2} A = i\gamma |A|^2 A$$

α is absorption, $\gamma = \dfrac{n_0 \omega_0}{c A_{eff}}$

where $n_2 = 3.2 \cdot 10^{-20}\ m^2/w$

ω_0 = carrier frequency

c = speed of light

A_{eff} = effective fiber core area

Also

$\beta_1 = \dfrac{1}{v_g}$ is v_g = group velocity

and

$\beta_2 = -\dfrac{1}{v_g^2}\dfrac{dv_g}{d\omega}$ is GVD

note: β_2 is related to the group delay dispersion $D(\lambda)$

$D = -\dfrac{2\pi c}{\lambda^2}\beta_2$ also $|D(\lambda)| = D(\lambda) \cdot c \cdot \lambda$

units: β_1 is in s/cm

β_2 is in ps^2/km

$D(\lambda)$ is in ps/km·nm

$|D(\lambda)|$ is unit less

3. Normalized propagation equation

$$i\frac{2}{\pi}\frac{\partial u}{\partial(z/z_0)} - \frac{1}{2}\frac{\partial^2 u}{\partial\tau^2} + N^2 e^{-\alpha z}|u|^2 u = 0$$

where

$$\tau = \frac{T}{T_0} = \frac{t - z/v_g}{T_0} ,$$

T_0 is input pulse width and

$$u(z,\tau) = \frac{1}{\sqrt{P_0}\exp\left(-\frac{\alpha z}{2}\right)} A(z,\tau)$$

P_0 is input pulse peak power and

$$N^2 = \frac{L_D}{L_{NL}} = \frac{\gamma P_0 T_0^2}{|\beta_2|} , L_D = \frac{T_0^2}{|\beta_2|} L_{NL} = \frac{1}{\gamma P_0}$$

and

$$z_0 = \frac{\pi}{2} L_D = \frac{\pi}{2}\frac{T_0^2}{\beta_2}$$

4. Design equations

$$z \simeq z_{opt}$$

Fiber length: $z_{opt} \simeq \frac{1.6}{N} \cdot z_0$

Slant length: $b_0 = \left\{\dfrac{\omega_0^3\, d^2 \cos^2 \gamma_0}{4\pi c}\right\} \dfrac{1.6}{N}\, T_0^2$

Compression factor: $\dfrac{T_0}{T_c} = \dfrac{1.6}{N}$

$z \ll z_{opt}$

Slant length: $b_0 = \dfrac{13}{84} \left\{\dfrac{\omega_0^3\, d^2 \cos^2 \gamma_0}{4\pi c}\right\} \dfrac{1.6}{N}\, \dfrac{z_0}{z}\, T_0^2$

Compression factor: $\dfrac{T_0}{T_c} \simeq 1 + .9\, N^2\, (z/z_0)$

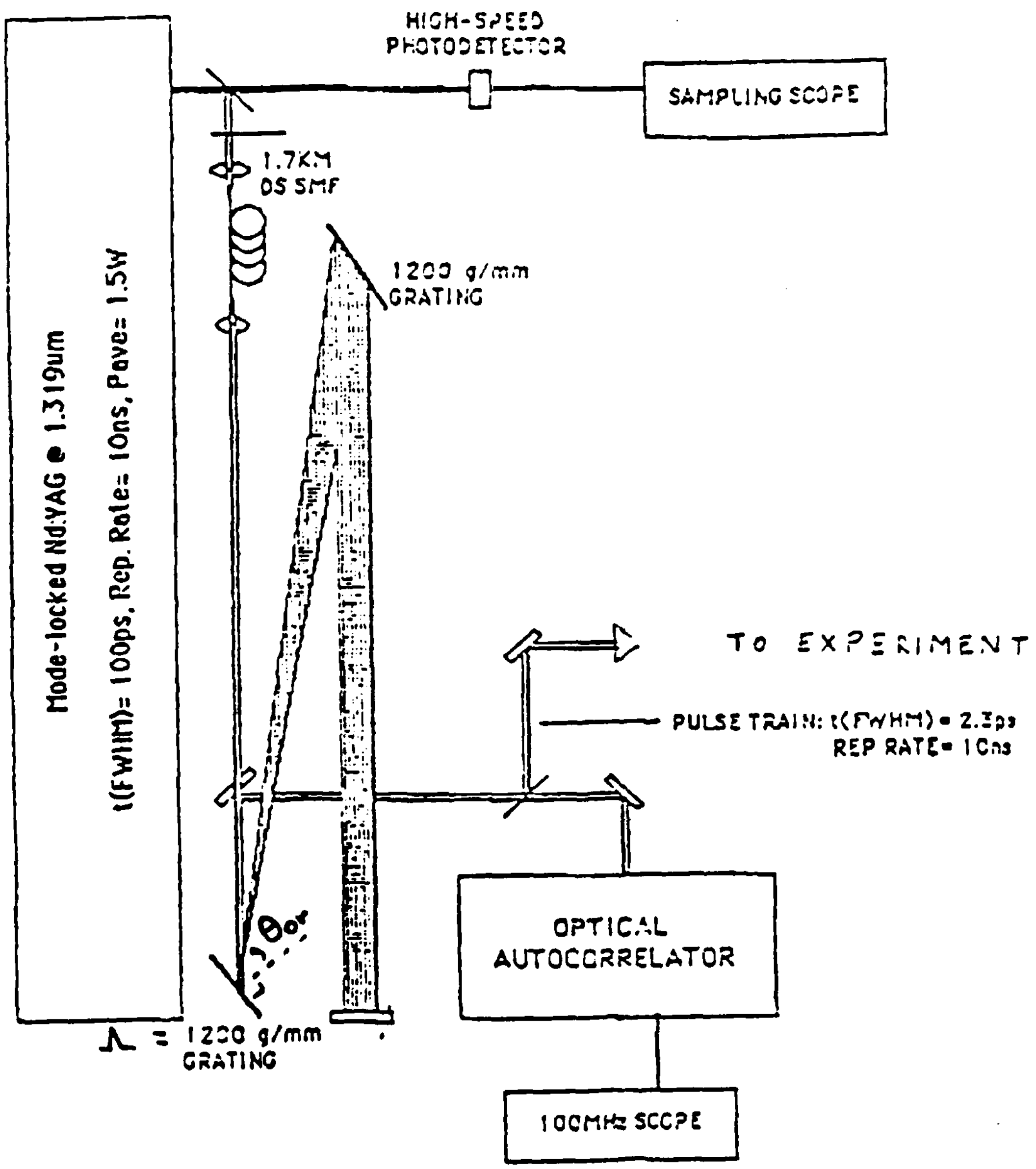

Figure 1. Pulse compression setup

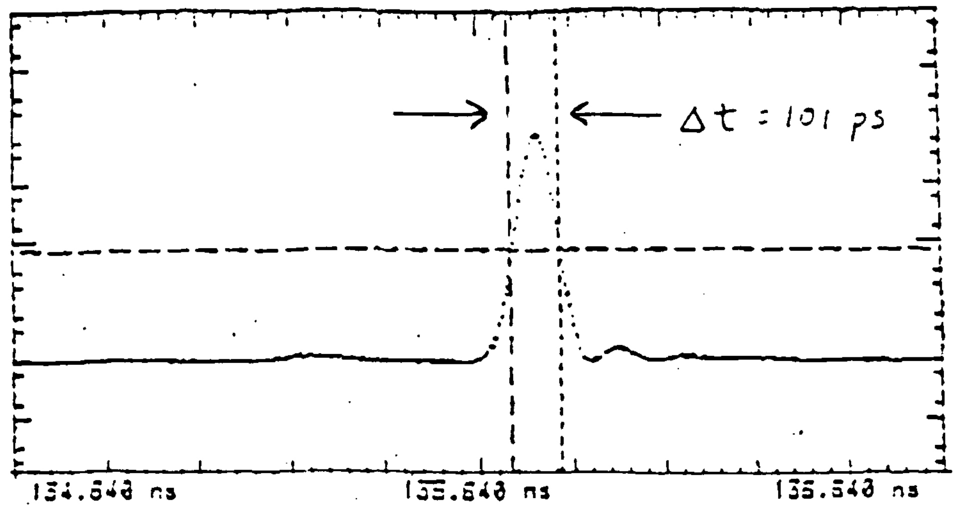

Figure 2. Input pulse: 101 ps

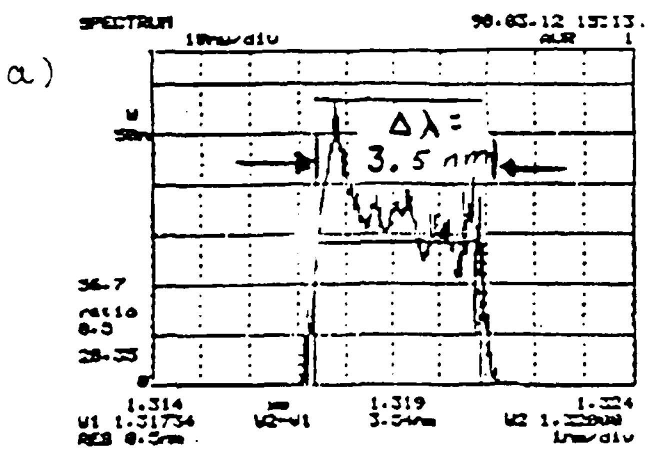

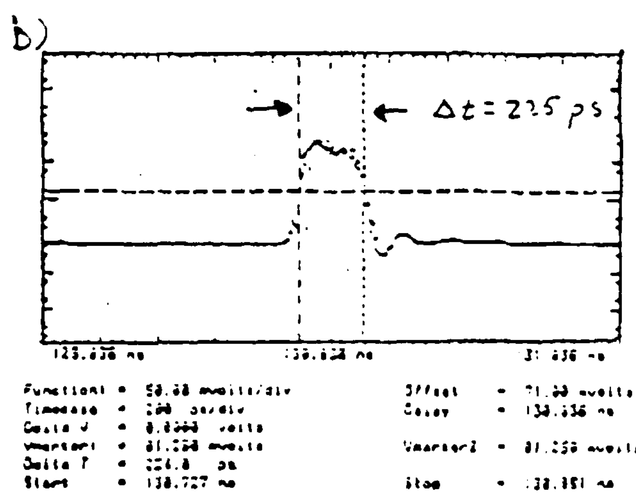

Figure 3. Output pulse after fiber:

a) Frequency spectrum, Δλ = 3.5 nm;

b) Temporal profile, Δt = 225 ps

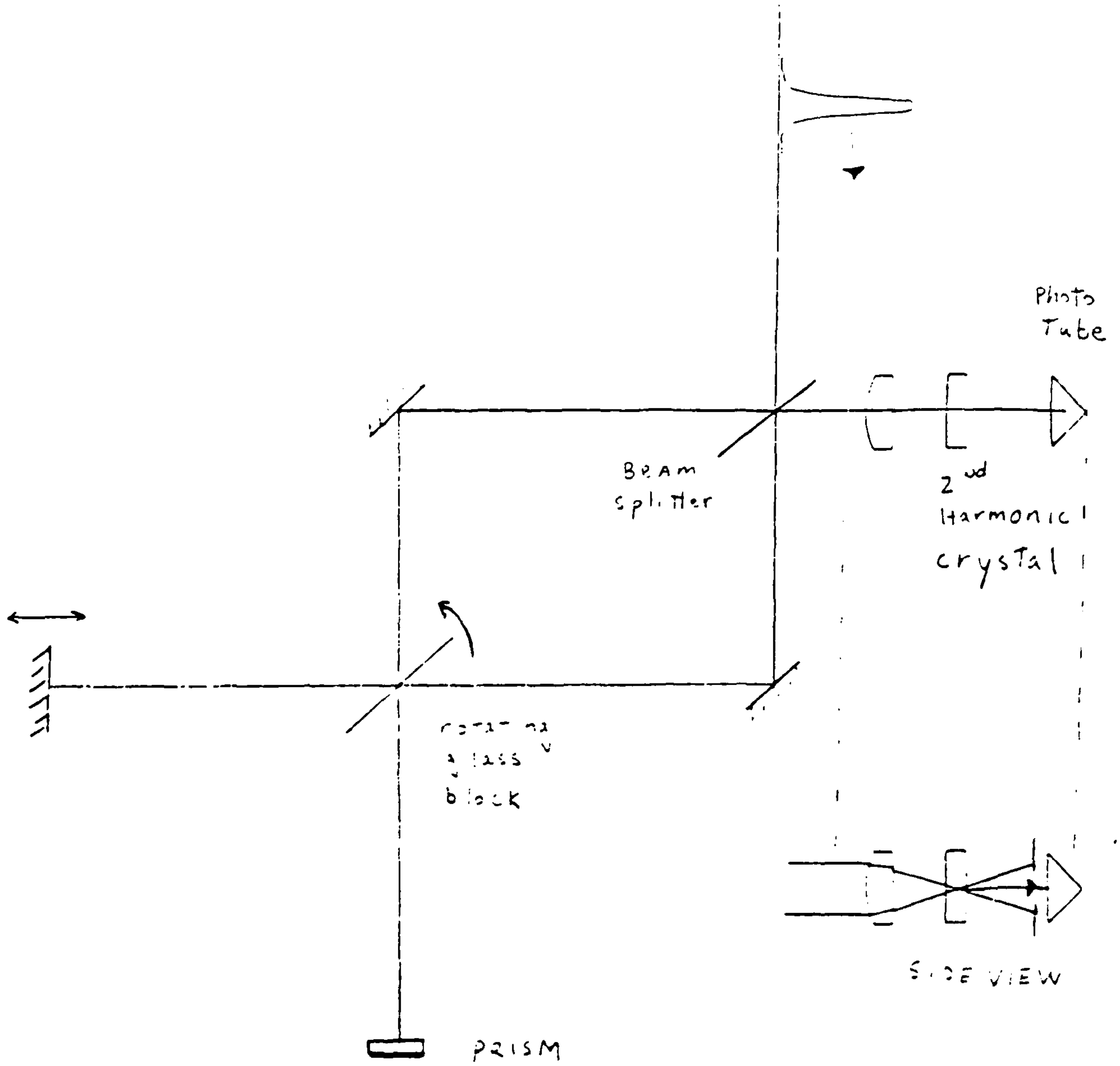

Figure 4. Autocorrelator

Parts Lists

The major components of both the pulse compressor and autocorrelator, along with some vendors, are listed below.

A. Pulse Compressor

part	vendor	#
(2) $\lambda/2$ plate @1.319um	CVI	
polarizer	CVI	
Fiber coupler	Newport	F-1015LD-DJ
Fiber coupler	Newport	F 916 T
Microscope objective	Newport	FL10B
"	Newport	FL20
Rotation stage	Control Optic	RS37A
Diffraction Gratings	Spectron	2" sq., 1200 gr/mm, 1.319um blaze
1.5 km Dispersion shifted fiber (1.55um)		Corning
(3) Mirror mounts	Newport	MM2

B. Autocorrelator

part	vendor	#
Color Filter	Oriel	51312
f = 50mm lens	Melles Griot	01 LPX 108
Beamsplitter	Ealing	356139
LiIO3 SHG crystal (in cell)	Inrad	10 deg. convergence angle
Mirror	Melles Griot	02 MFG 000, Al flat

Turning prism		
(1) 1" Mirror mount		
(1) 2" Mirror mount		
(4) iris diaphragm	Edmund Scientific	D30,263
Phototube	Hamamatsu	
Phototube Housing		
15V DC power supply for phototube		
2" x 1" x 3cm BK-7 glass flat		
Electric motor for glass block		
5V Power supply for electric motor		

MISSION
of
Rome Air Development Center

RADC plans and executes research, development, test and selected acquisition programs in support of Command, Control, Communications and Intelligence (C^3I) activities. Technical and engineering support within areas of competence is provided to ESD Program Offices (POs) and other ESD elements to perform effective acquisition of C^3I systems. The areas of technical competence include communications, command and control, battle management information processing, surveillance sensors, intelligence data collection and handling, solid state sciences, electromagnetics, and propagation, and electronic reliability/maintainability and compatibility.